# Self-Assembly of Insoluble Porphyrins on Au(111) under Aqueous Electrochemical Control

Sedigheh Sadegh Hassani,[†,‡] Youn-Geun Kim,[†] and Eric Borguet*,[†]

[†]Department of Chemistry, Temple University, Philadelphia, Pennsylvania 19122, United States
[‡]Nanotechnology Research Center, Research Institute of Petroleum Industry, Tehran, Iran

ABSTRACT: Self-assembled monolayers of a water-insoluble porphyrin, tetraphenyl porphyrin (TPP), in the presence of an aqueous electrolyte were characterized in situ with electrochemical scanning tunneling microscopy (EC-STM) at working electrode potentials of between 0.5 and −0.2 V. Isolated domains of TPP monolayers with differing orientation were observed on Au(111) in 0.1 M $HClO_4$ over this entire potential window. Individual TPP molecules could be resolved over a range of 700 mV, from open circuit potential (OCP) to near the hydrogen evolution potential. The unit cell is square, and the distance between neighboring molecules is about 1.4 ± 0.1 nm. High-resolution images allow the internal molecular structure to be discerned. No changes in the STM contrast of individual molecules were observed as the potential was changed. In a neutral electrolyte (0.1 M $KClO_4$, pH $\sim$6), the potential range of stability of ordered structures is reduced. On HOPG, TPP forms ordered hexagonal structures with a lattice constant of about 2.6 nm in the double-layer potential region in 0.1 M $HClO_4$.
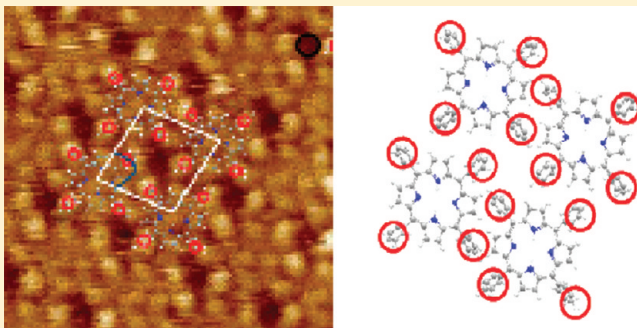
INTRODUCTION

Porphyrins are important components of many organic compounds found in biological systems.[1,2] For example, hemoglobin is a metalloprotein with a porphyrin structure at its core which is responsible for oxygen transport in the blood. Porphyrins have a flat, robust architecture.[3] They play an important role in the design of extended self-assembled adlayers of controlled size and shape. Porphyrins are of interest because of the versatile electronic and photonic properties,[4] a consequence of their structural flexibility,[5] and interesting redox properties.[6] The large number of fundamental surface science studies of ordered monolayers of porphyrins on single-crystal surfaces are driven in part by potential applications as active elements in optical devices,[7] chemical sensors,[8−10] solar cells,[11,12] functional supramolecular materials,[13] artificial photosynthesis, information storage,[14] and catalytic processes.[12]

In recent years, extensive studies have been performed on the self-assembly of organic molecules on surfaces.[15,16] Several techniques have been used to investigate porphyrins on surfaces: ultraviolet/visible absorption spectroscopy (UV/vis),[17,18] X-ray photoelectron spectroscopy (XPS),[19,20] cyclic voltammetry,[17,19] and scanning tunneling microscopy (STM).[12,13,21−23] These techniques make use of different physical principles to probe the monolayer and thus provide independent methods for the characterization of porphyrins on surfaces. STM, because it can provide atomic-scale images of adlayer molecules, has been used to characterize porphyrin derivatives in air,[22,24,25] under ultrahigh vacuum (UHV),[1,12,13,26−28] and under liquid[29−32] after deposition on different metal single-crystal surfaces[23,33−35] and highly
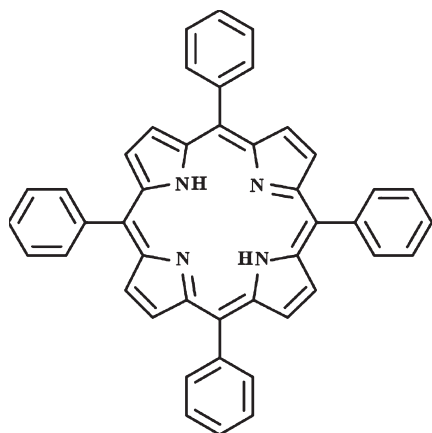
oriented pyrolytic graphite (HOPG).[1,13] STM images can be employed to determine the size and conformation of molecules on the surface as well as the lattice parameters of the ordered structures that they form.

Under electrochemical conditions, the electrode potential controls the excess charge on the electrode surface. This can alter the interactions between the surface and the electrolyte and solutes. Thus, the surface potential can play an important role in the ordering of adsorbates, in the adsorption or desorption of molecules on the electrode surface, and in redox reactions.[16,29−31] Electrochemical scanning tunneling microscopy (EC-STM) is a powerful technique for the study of electrified interfaces.[36] EC-STM allows the characterization of the topography of an electrode surface under potential control with atomic resolution enabling, for example, the investigation of electrochemical oxidation−reduction reactions at the single-molecule level at metal−electrolyte interfaces.[14,36−38]

An important goal of this report is to understand the adsorption of one of the simplest porphyrins, tetraphenylporphyrin (TPP) Figure 1, at the single-molecule level under electrochemical control. All previous publications related to STM studies of TPP monolayers were performed in UHV.[1,12,13,27,39,40] Although there has been tremendous progress in studying porphyrin self-assembly at solid−liquid interfaces with STM, there has been no detailed report of the metal-free tetraphenyl porphyrin (TPP). In this article, we present the first detailed investigation of TPP

Figure 1. Structure of tetraphenylporphyrin.

Figure 2. In situ STM images of the TPP-modified Au(111) electrode at 0.4 V in 0.1 M $HClO_4$ obtained over different areas of the bead with scales of (a) 35×35 nm^2 and (b) 50×50 nm^2. The image conditions are $E_{bias} = -0.3$ V and $I_t = 1$ nA. Small ordered domains (e.g., inside the white oval (a)) are observed.

Figure 3. STM images of the TPP-modified Au(111) electrode at 0.26 V in a 0.1 M $HClO_4$ solution with scales of (a) 50×50 nm^2 and (b) 20×20 nm^2. The image conditions are $E_{bias} = -0.17$ V and $I_t = 0.3$ nA.

self-assembly at a liquid−solid interface under potential control. (Previous studies reported, in the Supporting Information, the formation of small domains of TPP under electrochemical control without further details.[41]) We observed that TPP forms ordered structures over a wide range of potentials on Au(111) and on HOPG. We also report the effect of pH, which can change the charge state of the molecule and thereby the interactions with other molecules and with the surface.
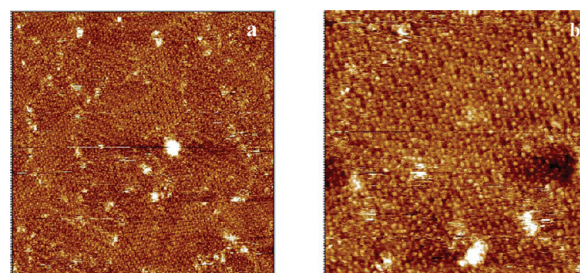
■ EXPERIMENTAL SECTION

A single-crystal gold bead was used as the substrate. Before all experiments, the substrate, the Teflon cell, the O-ring (Viton), the ceramic tweezers, and the Pt wires were cleaned by immersion in a hot piranha solution (1:3 H_2O_2 (J. T. Baker, CMOS)/H_2SO_4 (J. T. Baker, CMOS)) for 1 h. (*Caution! Piranha solution is a very strong oxidizing agent and is dangerous. Eye protection and gloves should be used during cleaning.*). Then they were rinsed by ultrasonication in ultrapure deionized (DI) water three times (>18 MΩ·cm, Barnstead, EasyPure system equipped with a UV lamp). Finally, a hydrogen flame was used to anneal the bead, followed by quenching in hydrogen-saturated ultrapure DI water (hydrogen flame annealing method[42]). The bead presented well-ordered Au(111) facets on which wide (>100 nm) terraces could be easily found.[14] 5,10,15,20-tetraphenyl-21*H*,23*H*-porphine (H_2TPP) was purchased from Sigma-Aldrich (purity 99%) and used without further purification. Self-assembled layers were prepared by immersing the gold bead into a TPP/benzene solution (20 μM) for 10 s and rinsing thoroughly with ultrapure water. Different concentrations and times were investigated, and these conditions were determined to be optimal for monolayer formation. Then the Au bead was promptly mounted into a Teflon electrochemical cell containing a 0.1 M $HClO_4$ (Fisher Scientific Co., trace metal grade) solution under potential control. The open circuit potential was measured to be around 0.45 V. All potentials are quoted against the saturated calomel electrode (SCE), though two platinum wires were used as counter and quasi-reference electrodes, respectively.

STM images were obtained with a PicoScan STM system (Molecular Imaging). STM tips were electrochemically etched (0.1 M KOH, ~15 V) from tungsten wire (Alfa Aesar, 0.25 mm in diameter), and the etched W wire was insulated with colorless nail polish. The faradaic current of the insulated tips under imaging conditions was typically less than 10 pA at experimental biases. All of the STM images were obtained in constant current mode (0.5−0.7 nA) with a high-resolution scanner and without further processing (e.g., high-pass filtering) except necessary image flattening. Tunneling conditions are reported in the respective figure captions. Molecular models were built and optimized with Chemoffice Ultra 2006 software (CambridgeSoft, Inc.).

■ RESULTS AND DISCUSSION

TPP Self-Assembly on Au(111) in $HClO_4$ Solution. After the STM tip was engaged, well-ordered small molecular domains of less than 10 nm immediately appeared at 0.4 V as shown in Figure 2. Similar images were observed in multiple locations on the surface. The TPP monolayer was observed to form domains of differing orientation on single Au(111) terraces. Three differently oriented TPP domains on the same Au terrace were found to be rotated by about 120° from one another. The boundaries between different domains are not clearly seen. However, molecular rows defining the domains are clearly seen in Figure 2a,b.

To investigate the possible formation of large molecular domains and the redox behavior of TPP, the potential was dropped in steps from 0.4 to 0.26 V. As a result, the fraction of the surface covered with ordered TPP domains increased and submolecular structure was clearly observed (Figure 3). It is apparent that the molecular array extends over the wide, atomically flat terrace of the Au(111) substrate with three differently oriented domains and that the surface is almost completely covered with TPP molecules. Despite the relatively large area of the image, each TPP molecule can be recognized within a slightly skewed array.

When the potential was changed to even more negative values (e.g., 0.23 V), well-ordered high-resolution images were distinctly observed. These structures and representative cross sections can be seen in Figure 4a−e.
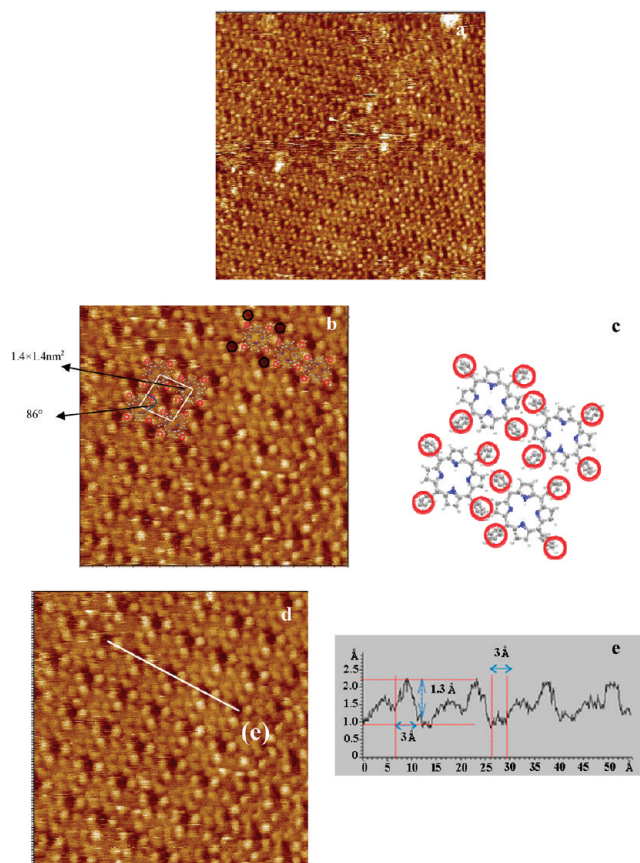
Figure 4. In situ high-resolution STM images, with submolecular resolution, of a TPP-modified Au(111) electrode at 0.23 V in 0.1 M HClO$_4$ with scales of (a) 20×20 nm^2 and (b, d) 10×10 nm^2. The image conditions are $E_{bias} = -0.14$ V and $I_t = 0.3$ nA. (c) Proposed TPP adlayer structure on Au(111). (e) Cross section of the TPP ordered structure acquired from the region under the white line labeled (e) in image d.

Each molecule can be identified as a square in Figure 4b,d. Four phenyl moieties of each TPP molecule can be individually recognized as four bright dots, each about 3 Å in diameter, forming the corners of the molecule. The shape of the molecule in the image clearly corresponds to the known chemical structure of the TPP molecule. A detailed assignment is proposed in Figure 4b, where the red circles indicate the tentative locations of the phenyl groups. A vertical cross section of the TPP ordered structure, from the region indicated by a white line on Figure 4d, is shown in Figure 4e. This reveals the diameter of the dark space between phenyl groups to be about 3 Å.

The suggestion that the phenyl units are more easily visible than the rest of the TPP molecule is supported by the expectation of the rotation of the phenyl units out of the molecular plane. The distance between neighboring molecules of about 1.4 ± 0.1 nm is in agreement with the TPP structure observed in UHV.[40] Molecular rows appear to cross each other at an angle of $\sim 86 \pm 1°$. On the basis of the high-resolution STM images, a tentative adlayer structure is proposed in Figure 4c.

To investigate the stability of the ordered TPP structures on Au(111) at even more negative potentials, the sample potential was lowered step by step to 0 V. In this process, it was noted that the ordered structure became more stable (Figure 5a−d, i.e., less perturbed by STM imaging even though the surface has been
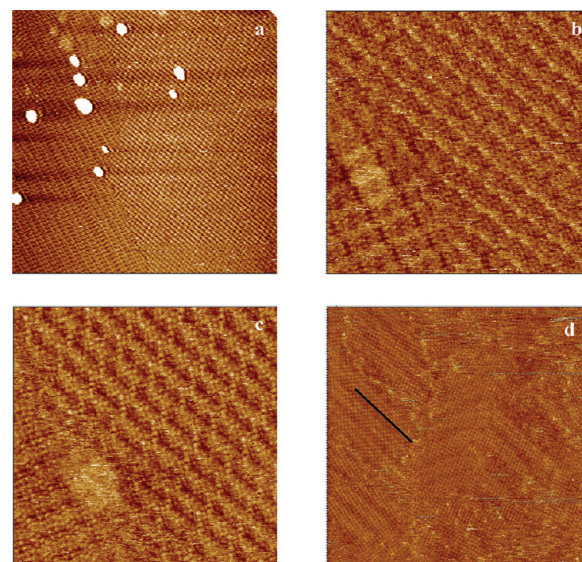

Figure 5. In situ STM image of TPP on a reconstructed Au(111) electrode surface in 0.1 M HClO$_4$ from 0.2 to 0 V. The image conditions are (a) $E_{bias} = -0.17$ V, $I_t = 0.8$ nA, and scan size 120×120 nm^2 at 0.2 V, (b) $E_{bias} = -0.17$ V, $I_t = 0.7$ nA, and scan size 20×20 nm^2 at 0.2 V, (c) $E_{bias} = -0.07$ V, $I_t = 0.7$ nA, and scan size 20×20 nm^2 at 0.1 V, and (d) $E_{bias} = 0.09$ V, $I_t = 0.3$ nA, and scan size 100×100 nm^2 at 0 V.
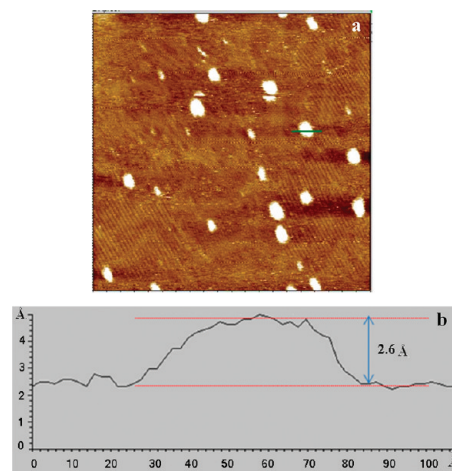
Figure 6. In situ STM image of TPP-modified Au(111) at −0.2 V in 0.1 M HClO$_4$. (a) Scan size 100×100 nm^2. (b) Cross section through one of the white dots ($E_{bias} = 0.29$ V and $I_t = 0.5$ nA.).

reconstructed. It should be noted that a lower tunneling current resulted in better resolution in these images.

The boundaries between differently oriented TPP domains are clearly seen on the underlying Au(111) surface reconstruction stripes, one of which is indicated by a black line in Figure 5d. It is clear that the molecular domains extend over the wide reconstructed terrace of the Au(111) substrate without any apparent influence from the changes in direction of the reconstruction stripes and that the surface is almost completely covered with TPP molecules. This result clearly shows that TPP forms very well ordered structures despite the surface reconstruction. In addition, it appears that the domain size increased as the potential was reduced.
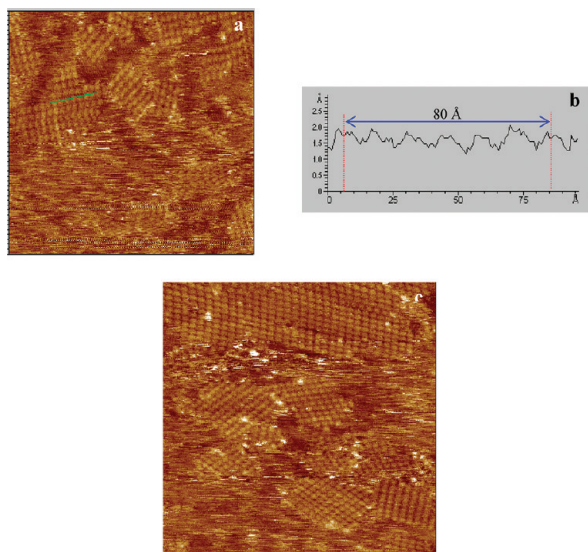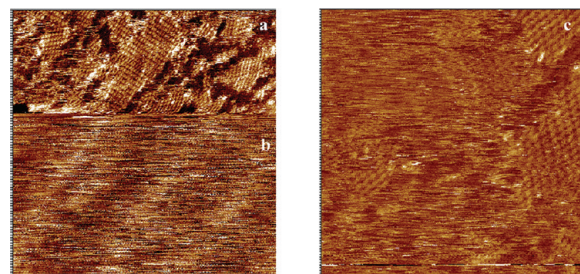
Figure 7. In situ STM image of a TPP-modified Au(111) electrode at 0.4 V in 0.1 M KClO$_4$ with scan sizes of (a) 50 × 50 nm^2 and (c) 45 × 45 nm^2. The image conditions are E_{bias} = −0.1 V and I_t = 0.3 nA. (b) Cross section of the ordered structure denoted by the line in image a.

Figure 8. Potential-dependent in situ STM images of a TPP-modified Au(111) electrode in 0.1 M KClO$_4$ with scan ranges of (a, b) 100 × 100 nm^2 and (c) 50 × 50 nm^2. The image conditions are (a, c) sample potential = 0.4 V, E_{bias} = −0.1 V, I_t = 0.3 nA and (b) sample potential = 0.2 V, E_{bias} = 0.1 V, and I_t = 0.3 nA.

Figure 9. In situ STM images of a TPP-modified HOPG electrode at 0.25 V in 0.1 M HClO$_4$ with scan ranges of (a) 100 × 100 nm^2 and (b) 30 × 30 nm^2. The image conditions are E_{bias} = −0.16 V and I_t = 0.7 nA. (c) Cross section of the TPP-ordered structure on HOPG under the line in the center of image a.

When the potential approached the hydrogen evolution region, the TPP adlayer became unstable and most ordered structures disappeared from the electrode surface (Figure 6), although several small ordered domains were locally observed at this potential, −0.2 V. A cross section through one of the white dots in Figure 6b shows that their height is around 2.6 Å. Because TPP is insoluble and islands due to the lifting of the Au(111) reconstruction are not expected at this potential, it is possible that the islands are aggregates of TPP molecules. Lowering the surface potential creates a more negatively charged metal surface and weakens the TPP−Au(111) interaction, probably because of the repulsive interaction between the TPP π-electron system and the negatively charged surface so that the adsorbed molecules become increasingly mobile, reducing the coverage of ordered domains. Furthermore, islands of aggregated molecules formed on the electrode surface because of interactions between the insoluble molecules that are no longer driven to interact strongly with the surface.

Changes in the STM contrast of adsorbed TPP molecules were not observed in the ordered domain in the potential range from −0.1 and −0.3 V, even though such phenomena were seen on the previous TPyP-,[6] TCCP-,[14] and Zn-TPP[41]-modified Au(111) surfaces in electrolyte.

TPP Self-Assembly on Au(111) in KClO$_4$ Solution. To investigate the pH dependence of the formation of ordered TPP structures, 0.1 M KClO$_4$ was used as an electrolyte to provide a solution at pH ∼6. After the STM tip was engaged, well-ordered domains immediately appeared at about 0.4 V as shown in Figure 7. Similar images were observed in multiple locations on the surface. A cross section of these ordered structures (Figure 7b) shows that the distance between neighboring molecules is about 1.4 ± 0.1 nm. Thus, it appears that TPP forms identical structures to those observed in 0.1 M HClO$_4$ solution.

The TPP monolayer was observed to form domains of differing orientation on Au(111) terraces. When changing to more negative potentials than 0.4 V, ordered structures were not
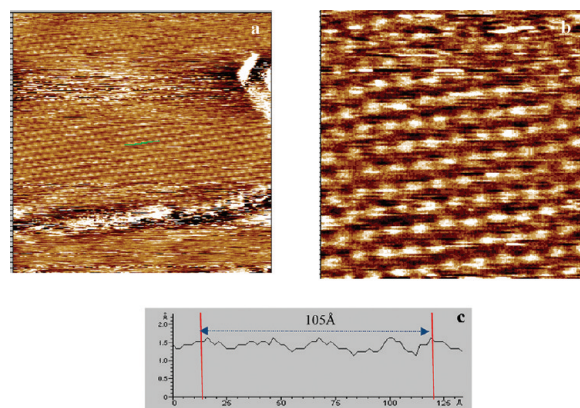
observed on Au(111) and no TPP molecules were observed on the surface. However, returning the potential to 0.4 V results again in the observation of ordered domains of TPP molecules. This is illustrated in Figure 8, where ordered TPP structures at 0.4 V are seen in the top part (a), but when the potential is abruptly changed to 0.2 V (bottom part of image labeled b), the ordered structure disappears. Returning the potential to 0.4 V results in the ordered structures reappearing (Figure 8c).

It appears that there is an order−disorder transition that is driven by the electrode potential, similar to what was observed for insoluble alkanes at electrified interfaces, where hexadecane molecules formed ordered lamellar structures at a potential near the pzc that disappeared at potentials that were sufficiently positive or negative.[43] It is interesting that the TPP adlayer is more stable under acidic rather that neutral conditions. One possible reason is that under acidic conditions TPP is protonated and therefore positively charged.

TPP Self-Assembly on HOPG. To investigate the effect of the substrate, a TPP-covered HOPG surface was prepared in a manner similar to that of TPP-covered Au(111). After the STM tip was engaged, well-ordered domains could not be seen immediately. After about 1 h, some ordered domains appeared at 0.25 V as shown in Figure 9a,b. Similar images were observed in multiple locations on the surface. The STM image clearly shows that the resulting hexagonal packing geometries and unit cell are

different from the TPP-ordered structures on Au(111). The cross section shown in Figure 9c, obtained from Figure 9a (green line), suggests that the distance between neighboring molecules is about 2.6 nm. Similar hexagonal arrays of TPP on HOPG in UHV have been reported, but with a somewhat larger lattice constant (3.2 nm).[1,13]

Although similar patterns were observed in the UHV study, a detailed explanation of this observation was not given. This result suggests that self-assembled TPP molecule coverage on HOPG is less than its coverage on the Au(111) electrode. It seems that the interactions between TPP molecules and HOPG are weaker than with the Au(111) surface. Interestingly, the potential range over which ordered TPP structures were observed on HOPG in 0.1 M $HClO_4$ was considerably reduced. In the limited experiments performed, ordered structures were observed only near 0.25 V.

■ CONCLUSIONS

Electrochemical STM was used to image tetraphenyl porphyrin (TPP) on Au(111) in the presence of aqueous electrolyte. High-resolution STM images of TPP were obtained under solvent and electrochemical control at working electrode potentials of between 0.5 and −0.2 V. Isolated domains with differing orientation, in which individual TPP molecules could be identified, were observed over a range of 700 mV, from open circuit potential (OCP) to near hydrogen evolution potential. In comparison with other TPP-monolayer STM images acquired in UHV, the present work shows high-quality STM images under electrochemical conditions with a simple nearly square unit cell with a lattice parameter of 1.4 ± 0.1 nm. High-resolution images allow the internal molecular structure to be discerned. At nearly neutral pH in 0.1 M $KClO_4$ (pH ∼6), similar ordered structures and domains were seen, but only in a narrow potential range near 0.4 V. At more negative potentials, the ordered structure disappears but could be recovered by returning to 0.4 V, suggesting a reversible order−disorder transition that is driven by the electrode potential. The self-assembly of TPP on HOPG under potential control was observed by STM, clearly showing a hexagonal unit cell that is different from TPP-ordered structures on Au(111).

■ AUTHOR INFORMATION

Corresponding Author
*E-mail: eborguet@temple.edu.

■ ACKNOWLEDGMENT

■ REFERENCES

(1) Scarselli, M.; Ercolani, G.; Castrucci, P.; Monti, D.; Bussetti, G.; Russo, M.; Goletti, C.; Chiaradia, P.; Paolesse, R.; De Crescenzi, M. *Surf. Sci.* **2007**, *601*, 2607.
(2) Sessler, J. L.; Cyr, M.; Furuta, H.; Kral, V.; Mody, T.; Morishima, T.; Shionoya, M.; Weghorn, S. *Pure Appl. Chem.* **1993**, *65*, 393.
(3) Brede, J.; Linares, M.; Lensen, R.; Rowan, A. E.; Funk, M.; Broring, M.; Hoffmann, G.; Wiesendanger, R. *J. Vac. Sci. Technol., B* **2009**, *27*, 799.
(4) Dilung, I. I.; Kapinus, E. I. *Usp. Khimii.* **1978**, *47*, 83.
(5) Qiu, X. H.; Nazin, G. V.; Ho, W. *Phys. Rev. Lett.* **2004**, *93*, 4.
(6) He, Y.; Borguet, E. *Angew. Chem., Int. Ed.* **2007**, *46*, 6098.
(7) Debreczeny, M. P.; Svec, W. A.; Wasielewski, M. R. *Science* **1996**, *274*, 584.
(8) Lee, S. K.; Okura, I. *Anal. Chim. Acta* **1997**, *342*, 181.
(9) Lee, S. K.; Okura, I. *Analyst* **1997**, *122*, 81.
(10) Paolesse, R.; Di Natale, C.; Dall'Orto, V. C.; Macagnano, A.; Angelaccio, A.; Motta, N.; Sgarlata, A.; Hurst, J.; Rezzano, I.; Mascini, M.; D'Amico, A. *Thin Solid Films* **1999**, *354*, 245.
(11) Armel, V.; Pringle, J. M.; Forsyth, M.; MacFarlane, D. R.; Officer, D. L.; Wagner, P. *Chem. Commun.* **2010**, *46*, 3146.
(12) Buchner, F.; Flechtner, K.; Bai, Y.; Zillner, E.; Kellner, I.; Steinruck, H. P.; Marbach, H.; Gottfried, J. M. *J. Phys. Chem. C* **2008**, *112*, 15458.
(13) Scarselli, M.; Castrucci, P.; Monti, D.; De Crescenzi, M. *Surf. Sci.* **2007**, *601*, 5526.
(14) Yuan, Q. H.; Xing, Y. J.; Borguet, E. *J. Am. Chem. Soc.* **2010**, *132*, 5054.
(15) Buchner, F.; Warnick, K. G.; Wolfle, T.; Gorling, A.; Steinruck, H. P.; Hieringer, W.; Marbach, H. *J. Phys. Chem. C* **2009**, *113*, 16450.
(16) Elemans, J.; Van Hameren, R.; Nolte, R. J. M.; Rowan, A. E. *Adv. Mater.* **2006**, *18*, 1251.
(17) Imahori, H.; Norieda, H.; Ozawa, S.; Ushida, K.; Yamada, H.; Azuma, T.; Tamaki, K.; Sakata, Y. *Langmuir* **1998**, *14*, 5335.
(18) Postlethwaite, T. A.; Hutchison, J. E.; Hathcock, K. W.; Murray, R. W. *Langmuir* **1995**, *11*, 4109.
(19) Kondo, T.; Ito, T.; Nomura, S.; Uosaki, K. *Thin Solid Films* **1996**, *284*, 652.
(20) Shimazu, K.; Takechi, M.; Fujii, H.; Suzuki, M.; Saiki, H.; Yoshimura, T.; Uosaki, K. *Thin Solid Films* **1996**, *273*, 250.
(21) Buchner, F.; Kellner, I.; Steinruck, H. P.; Marbach, H. *Z. Phys. Chem.* **2009**, *223*, 131.
(22) Qiu, X. H.; Wang, C.; Zeng, Q. D.; Xu, B.; Yin, S. X.; Wang, H. N.; Xu, S. D.; Bai, C. L. *J. Am. Chem. Soc.* **2000**, *122*, 5550.
(23) Suto, K.; Yoshimoto, S.; Itaya, K. *J. Nanosci. Nanotechnol.* **2009**, *9*, 288.
(24) Ogunrinde, A.; Hipps, K. W.; Scudiero, L. *Langmuir* **2006**, *22*, 5697.
(25) Wang, H. N.; Wang, C.; Zeng, Q. D.; Xu, S. D.; Yin, S. X.; Xu, B.; Bai, C. L. *Surf. Interface Anal.* **2001**, *32*, 266.
(26) Gimzewski, J. K.; Joachim, C.; Schlittler, R. R.; Langlais, V.; Tang, H.; Johannsen, I. *Science* **1998**, *281*, 531.
(27) Grill, L.; Dyer, M.; Lafferentz, L.; Persson, M.; Peters, M. V.; Hecht, S. *Nat. Nanotechnol.* **2007**, *2*, 687.
(28) Ikeda, T.; Asakawa, M.; Goto, M.; Miyake, K.; Ishida, T.; Shimizu, T. *Langmuir* **2004**, *20*, 5454.
(29) Hulsken, B.; van Hameren, R.; Thordarson, P.; Gerritsen, J. W.; Nolte, R. J. M.; Rowan, A. E.; Crossley, M. J.; Elemans, J.; Speller, S. *Jpn. J. Appl. Phys., Part 1* **2006**, *45*, 1953.
(30) Kunitake, M.; Akiba, U.; Batina, N.; Itaya, K. *Langmuir* **1997**, *13*, 1607.
(31) Kunitake, M.; Batina, N.; Itaya, K. *Langmuir* **1995**, *11*, 2337.
(32) Tao, N. J.; Cardenas, G.; Cunha, F.; Shi, Z. *Langmuir* **1995**, *11*, 4445.
(33) Auwarter, W.; Weber-Bargioni, A.; Brink, S.; Riemann, A.; Schiffrin, A.; Ruben, M.; Barth, J. V. *ChemPhysChem* **2007**, *8*, 250.
(34) Bai, Y.; Buchner, F.; Kellner, I.; Schmid, M.; Vollnhals, F.; Steinruck, H. P.; Marbach, H.; Gottfried, J. M. *New J. Phys.* **2009** *11*, 15.
(35) Zotti, L. A.; Teobaldi, G.; Hofer, W. A.; Auwarter, W.; Weber-Bargioni, A.; Barth, J. V. *Surf. Sci.* **2007**, *601*, 2409.
(36) Itaya, K. *Prog. Surf. Sci.* **1998**, *58*, 121.
(37) He, Y.; Ye, T.; Borguet, E. *J. Am. Chem. Soc.* **2002**, *124*, 11964.
(38) Thorgaard, S. N.; Buhlmann, P. *Langmuir* **2010**, *26*, 7133.
(39) Grill, L. *J. Phys.: Condens. Matter* **2008**, *20*, 19.
(40) Rojas, G.; Chen, X.; Bravo, C.; Kim, J. H.; Kim, J. S.; Xiao, J.; Dowben, P. A.; Gao, Y.; Zeng, X. C.; Choe, W.; Enders, A. *J. Phys. Chem. C* **2010**, *114*, 9408.

(41) Yoshimoto, S.; Tsutsumi, E.; Suto, K.; Honda, Y.; Itaya, K. *Chem. Phys.* **2005**, *319*, 147.

(42) Clavilier, J.; Faure, R.; Guinet, G.; Durand, R. *J. Electroanal. Chem.* **1980**, *107*, 205.

(43) He, Y. F.; Ye, T.; Borguet, E. *J. Phys. Chem. B* **2002**, *106*, 11264.